Amylose is synthesized in vitro by extension of and cleavage from amylopectin

Marion van de Wal, Christophe d'Hulst, Jean-Paul Vincken, Alain Buleon, Richard Visser, Steven Ball

THE JOURNAL OF BIOLOGICAL CHEMISTRY
Vol. 273, No. 35, Issue of August 28, pp. 22232–22240, 1998

Printed in U.S.A.

Amylose Is Synthesized *in Vitro* by Extension of and Cleavage from Amylopectin*

(Received for publication, February 17, 1998, and in revised form, April 30, 1998)

Marion van de Wal‡, Christophe D'Hulst§, Jean-Paul Vincken‡, Alain Buléon¶, Richard Visser‡, and Steven Ball§‖

From the §Laboratoire de Chimie Biologique, Unité Mixte de Recherche du CNRS no. 111, Université des Sciences et Technologies de Lille, 59655 Villeneuve d'Ascq Cedex, France, ¶Institut National de la Recherche Agronomique, Centre de Recherches Agroalimentaires, Rue de la Géraudière, B.P. 71627, 44316 Nantes Cedex 03, France, and the ‡Department of Plant Breeding, Graduate School of Experimental Plant Sciences, Agricultural University of Wageningen, P. O. Box 386, 6700 AJ Wageningen, The Netherlands

Amylose synthesis was obtained *in vitro* from purified *Chlamydomonas reinhardtii* starch granules. Labeling experiments clearly indicate that initially the major granule-bound starch synthase extends glucans available on amylopectin. Amylose synthesis occurs thereafter at rates approaching or exceeding those of net polysaccharide synthesis. Although these results suggested that amylose originates from cleavage of a pre-existing external amylopectin chain, such transfer of chains from amylopectin to amylose was directly evidenced from pulse-chase experiments. The structure of the *in vitro* synthesized amylose could not be distinguished from *in vivo* synthesized amylose by a variety of methods. Moreover high molecular mass branched amylose synthesis preceded that of the low molecular mass, suggesting that chain termination occurs consequently to glucan cleavage. Short pulses of synthesis followed by incubation in buffer with or without ADP-Glc prove that transfer requires the presence of the glucosyl-nucleotide. Taken together, these observations make a compelling case for amylopectin acting as the *in vivo* primer for amylose synthesis. They further prove that extension is followed by cleavage. A model is presented that can explain the major features of amylose synthesis in plants. The consequences of intensive amylose synthesis on the crystal organization of amylopectin are reported through wide angle x-ray analysis of the *in vitro* synthesized polysaccharides.

Starch is usually defined as a mix of two distinct polymer fractions: amylopectin and amylose. Amylopectin the major compound is composed of intermediate size $\alpha(1\rightarrow4)$-linked glucans that are organized in clusters of parallel chains by a dense packing of $\alpha(1\rightarrow6)$ linkages. Amylose, which accounts for 20–30% in weight of the starch granule, is often referred to as a smaller linear molecule with very few $\alpha(1\rightarrow6)$ branches (for review, see Ref. 1). It has been apparent ever since the pioneering work of Leloir and Recondo (2, 3) that glucose is transferred from ADP-Glc to the nonreducing end of a growing $\alpha(1\rightarrow4)$-linked glucan, thus coupling an extra glucose residue to this chain with the simultaneous release of ADP.

The enzyme was identified by Fekete *et al.* (4) as associated with starch granules and was subsequently called granule-bound starch synthase. Due to the position of GBSSI[1] inside the granule, diffusion of both donor and acceptor substrate might be a limiting factor for activity. GBSSI was first reported to use non-physiological concentrations of UDP-Glc (2), whereas ADP-Glc was shortly discovered thereafter as the preferred donor substrate (3). These observations opened an altogether new area of research for both glycogen and starch synthesis in bacteria and plants, respectively. It has been known, ever since the foundation work laid by Nelson and Rines (5), that GBSSI is responsible for the biosynthesis of the amylose fraction. Mutations leading to defects for GBSSI have been isolated in an ever increasing number of species including *waxy* (*wx*) maize (6), *wx* rice (7), *wx* barley (8), *wx* wheat (9), amylose-free (*amf*) potato (10), low amylose (*lam*) pea (11), *wx* amaranth (12), and *sta2 Chlamydomonas reinhardtii* (13). All mutants accumulate during storage normal amounts of starch granules containing amylopectin with wild-type crystalline organization (14). These important results establish that amylose is not required for the biogenesis of normal granules. A number of studies approaching the synthesis of amylose *in vitro* (2, 15-17), establish that GBSSI incorporates glucose both in amylopectin and amylose according to the conditions used. *In vivo* evidence supporting the involvement of GBSSI in amylopectin synthesis was produced by Maddelein *et al.* (18). In this study, genetic interaction experiments clearly showed that defects in GBSSI strongly reduced amylopectin synthesis in particular mutant backgrounds.

We have shown that growth-arrested (nitrogen-starved) *C. reinhardtii* cells accumulate a polysaccharide that bears strong structural resemblance to maize endosperm storage starch (13, 18, 19). Moreover, we have demonstrated that similar enzymes synthesize it and that it responds in an identical fashion to mutations affecting these activities (12, 20). We have reported that the starch accumulated during log-phase growth differs markedly from storage starch (21). The polysaccharide, which is similar to vascular plant leaf (transient) starch, harbors little or no amylose whereas the amylopectin displays an altered chain-length distribution. Van den Koornhuyse *et al.* (22) showed that, in *C. reinhardtii,* mutants defective either for

* This work was supported by the European Union FAIR program (CT-95–0568); by the European Union AMICA program; by Université des Sciences et Technologies de Lille; by the Ministère de l'Education Nationale; by CNRS (Unité Mixte de Recherche du CNRS no. 111; Director André Verbert); by the Ministry of Economic Affairs, the Ministry of Education, Culture and Sciences, and the Ministry of Agriculture, Nature Management and Fishery in the framework of an industrial relevant research program of the Netherlands Association of Biotechnology Centers in the Netherlands; and by EU Short Term Training Fellowship PTP107. The costs of publication of this article were defrayed in part by the payment of page charges. This article must therefore be hereby marked "*advertisement*" in accordance with 18 U.S.C. Section 1734 solely to indicate this fact.

‖ To whom correspondence should be addressed. Tel.: 33-3-20-43-65-43; Fax: 33-3-20-43-65-55; E-mail: steven.ball@univ-lille1.fr.

[1] The abbreviations used are: GBSSI, granule-bound starch synthase I; BE, branching enzyme; λ_{max}, maximal absorbance wavelength of the iodine-polysaccharide complex.

phosphoglucomutase or for the large subunit of ADP-Glc pyrophosphorylase accumulate, under storage conditions, polysaccharides whose structure were identical to those of transient starch. Transient starch structures are those naturally found in plant storage organs prior to storage starch and consequently amylose biosynthesis. Storage starch extracted from mutants defective for ADP-Glc supply together with transient starches extracted from wild-type algae offer a unique opportunity to study the biosynthesis of amylose *in vitro*. Indeed, prior to their incubation with ADP-Glc, these starches contain virtually no amylose (21, 22). In addition, the reported levels of GBSSI activity and protein increased 4–5-fold with respect to those found for storage starches. Following the *in vitro* synthesis experiments reported in this paper, we propose an entirely new mechanism for amylose synthesis in plants.

EXPERIMENTAL PROCEDURES

Materials—ADP[U-^{14}C]Glc was purchased from Amersham (United Kingdom). ADP-Glc, maize amylopectin, potato amylose, potato starch, sweet potato β-amylase, Pronase, and proteinase K were obtained from Sigma. Amyloglucosidase maltose and maltotriose were obtained from Boehringer Mannheim (Mannheim, Germany). *Pseudomonas amyloderamosa* isoamylase was purchased from Hayashibara Biochemical Laboratories (Okayama, Japan).

Chlamydomonas Strains, Growth Conditions, and Media—The reference strain of *C. reinhardtii* used in this study is 137C (*mt*$^-$ *nit1 nit2*). I7, defective for the large subunit of ADP-Glc pyrophosphorylase (*sta1–1*), was generated by x-ray mutagenesis from 137C and has been described previously (20). The GBSSI-defective strain BAFR1 (*mt*$^+$ *nit1 nit2 sta2–29:ARG7*) contains a disruption of the *STA2* gene that was generated through random integration of the pARG7 plasmid in the nuclear DNA of *C. reinhardtii* (17). Standard media are fully detailed in Ref. 23, while growth conditions and nitrogen-starved media are described in Refs. 13, 20, 21, and 24.

Determination of Amylopectin/Amylose Content, Starch Purification, and Spectral Properties of the Iodine-Starch Complex—A full account of amyloglucosidase assays, starch purification on Percoll gradients, and λ_{max} determinations can be found in Ref. 13.

In Vitro Synthesis of Amylose, Protease Protection Experiments—500 μg of starch was incubated with 3.2 mM ADP-Glc in the presence of 50 mM glycine (pH 9.0), 100 mM $(NH_4)_2SO_4$, 0.4% β - mercaptoethanol, 5 mM $MgCl_2$, 0.05% bovine serum albumin, and 2.2 μM ADP[U-^{14}C]Glc at 10.5 GBq/mmol in a total volume of 2 ml at 30 °C for different periods of time. The reaction was terminated by adding three volumes of 96% ethanol. After centrifugation at 3000 × *g* for 10 min, the supernatant was discarded and the starch was suspended in 100% Me_2SO and boiled for 20 min. The polysaccharide was precipitated overnight at – 20 °C by adding three volumes of 96% ethanol. After centrifugation at 15,000 × *g* for 20 min at 4 °C, the pellet was dried in air for at least 10 min, dissolved in 500 μl of 10 mM NaOH, and subjected to gel permeation chromatography. To investigate the sensitivity of GBSSI to proteases, concentrations of 0.1 and 0.2 mg·ml^{-1} were used, respectively, for proteinase K and Pronase using the standard GBSSI assays at 30 min and 1 h after a 30-min preincubation.

Separation of Starch Polysaccharides by Gel Permeation Chromatography—0.5–1.0 mg of starch dissolved in 500 μl of 10 mM NaOH was applied to a column (0.5 cm (inner diameter) × 65 cm) of Sepharose CL2B or CL4B, which was equilibrated and eluted with 10 mM NaOH. Fractions of 300–320 μl were collected at a rate of one fraction per 1.5 min. Radioactivity was determined by liquid scintillation counting. Glucans in the fractions were detected by their reaction with iodine, and the levels of amylopectin and amylose were quantified by determining the amount of glucose after amyloglucosidase treatment.

Debranching Analysis—Isoamylase-mediated debranching of gel permeation chromatography-purified fractions of amylopectin and amylose was achieved as described previously (21). After completion of the debranching reaction, samples were kept at 80 °C in 10% Me_2SO to avoid retrogradation of the long glucans into insoluble material. The debranched polysaccharides were subjected to TSK HW-50(F) chromatography as detailed in Ref. 21. Debranching of amylopectin for CL4B gel permeation chromatography was performed in 50 mM NaAc (pH 4.0) containing 59 units of isoamylase.

Determination of the β-Amylolysis Limit—Amylose and amylopectin were dissolved in 25 μl of 0.8 M NaOH, diluted with 25 μl of distilled water and incubated for 24 h at 30 °C in 200 μl of 50 mM NaAc (pH 3.5). The latter contained no β-amylase, 22 units of β-amylase, or both 22 units of β-amylase and 59 units of isoamylase. After adding 150 μl of 3,5-dinitrosalicylic acid (10 mg·ml^{-1}) to 50 μl of sample, the mixture was boiled for 10 min and the number of reducing ends was determined spectrophotometricaly at 540 nm. Maltose was used as a standard. As a control, the β-amylolysis limit was determined for maize amylopectin, potato amylose, and potato starch.

X-ray Diffraction Measurements—Samples (10 mg) were sealed between two aluminum foils, to prevent any significant change in water content during the measurement. Diffraction diagrams were recorded using Inel (Orléans, France) x-ray equipment operating at 40 kV and 30 mA. Cu$K_{\alpha 1}$ radiation (l = 0.15405 nm) was selected using a quartz monochromator. A curved position-sensitive detector (Inel CPS120) was used to monitor the diffracted intensities using 2-h exposure periods. Relative crystallinity was determined, after bringing all recorded diagrams at the same scale using normalization of the total scattering between 3 and 30° (2Θ), following a method derived from Wakelin *et al.* (26). Dry extruded starch and spherolitic crystals of amylose were used as amorphous and crystalline standards, respectively.

RESULTS

Synthesis of Amylose Occurs in Vitro from Transient Starches in the Absence of Added Maltooligosaccharides—Starch was purified both from nitrogen-starved cultures of mutants defective for the large subunit of ADP-Glc pyrophosphorylase and from nitrogen supplied wild-type algae. The granules extracted from these strains displayed GBSSI activities ranging between 15 and 20 nmol of ADP-Glc incorporated into insoluble polysaccharide per min and per mg of starch. This activity displayed an apparent K_m of 3.5 mM for ADP-Glc and was entirely protected from Pronase (0.2 mg·ml^{-1}) and (or) proteinase K (0.1 mg·ml^{-1}) action. When using 3.2 mM ADP-Glc, incorporation was linear with time for periods ranging from 10 min to 2 h at 30 °C. Although all experiments reported in this paper were performed from freshly purified material, no loss of GBSSI activity could be evidenced after 1 week of storage at 4 °C. Starch purified from strain BAFR1 (containing a gene-disrupted GBSSI structural gene) displayed less than 0.5% of the wild-type activity, which fell below background when fractionated on Sepharose CL2B columns. This proves that only GBSSI was monitored under our experimental conditions. Fig. 1 (*A* and *B*) shows the separation of amylopectin and amylose by CL2B chromatography before and after *in vitro* synthesis, respectively. After 24 h, we were able to raise the amylose content from less than 2% to over 24% of the total starch. The polysaccharide synthesized under these conditions could not be distinguished from standard *C. reinhardtii* amylose. Fig. 1*C* displays an experiment where 0.05 mg of starch subjected to *in vitro* synthesis for 24 h in the presence of labeled ADP-Glc was mixed and chromatographed with 1 mg of storage starch (20% amylose) extracted from wild-type cultures. We can conclude from these experiments that the molecular mass distribution of the *in vitro* synthesized material is identical to that of native amylose. Moreover, the fine structure of the *in vitro* synthesized product was investigated using debranching analysis followed by gel permeation (Fig. 2*A*). By all these criteria, the *in vitro* synthesized polysaccharide proved to be identical to native *C. reinhardtii* amylose. As with algal native amylose, we detected up to 1% branches within the *in vitro* synthesized product. We confirmed the presence of a similar branching pattern by measuring the β-amylolysis limit. β-Amylase is known to be an exo-type of enzyme digesting external chains up to 2–3 residues from a branch point. The β-amylolysis limit (the percentage of digested material) for both the *in vitro* and *in vivo* synthesized amyloses ranged between 70 and 75%. Together with the identical chain-length distributions revealed by our debranching analyses (see above), these results prove that both polysaccharides contain an identical distribution of α(1→6) linkages with a strong bias toward the reducing end of the molecules (for review, see Ref. 25). From all these

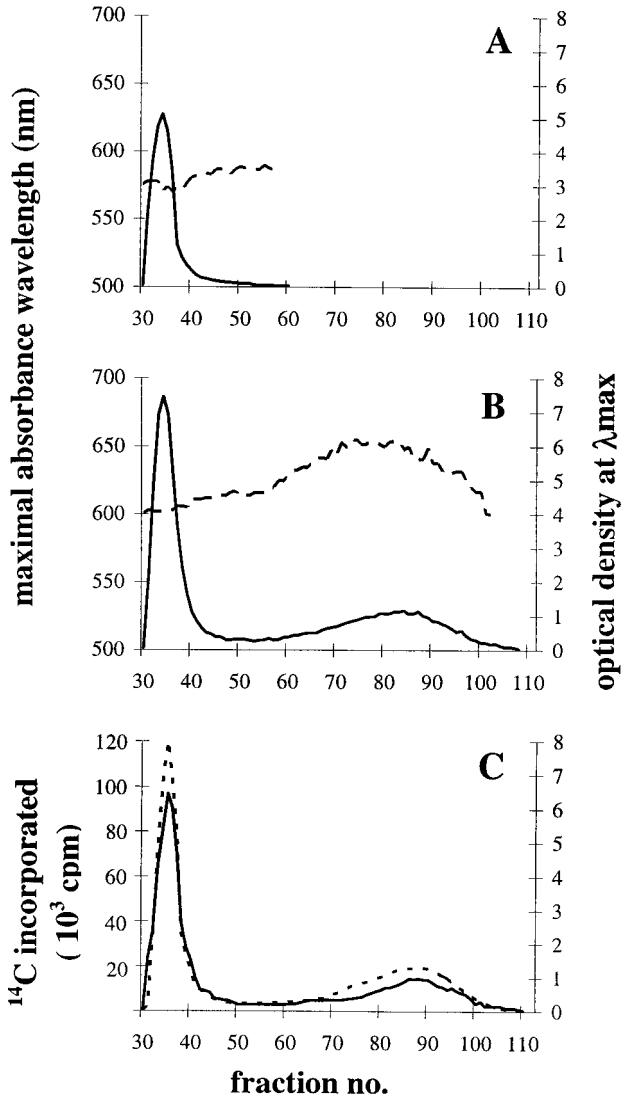

FIG. 1. **Separation of amylopectin and amylose by CL2B-Sepharose chromatography.** The optical density (——) of the iodine-polysaccharide complex was measured at λ_{max} (- - -) before (*A*) and after (*B*) 24 h of *in vitro* synthesis. The starch extracted from the mutant defective for the large subunit of ADP-Glc pyrophosphorylase (I7) displayed no detectable amounts of amylose (*A*). After 24 h of *in vitro* synthesis, the amylose content rose to over 24% of the total starch (*B*). *C* displays the optical density (——) and the incorporation of ^{14}C from ADP[U-^{14}C]Glc (- - -) after mixing 1 mg of wild-type storage starch and 0.05 mg of I7 starch subjected to 24 h of *in vitro* synthesis. The radioactivity was determined by liquid scintillation counting. Because of the relative abundance of cold wild-type reference polysaccharides, the OD reflects exclusively the wild-type amylopectin and amylose, whereas the radioactive material represents the *in vitro* synthesized glucans.

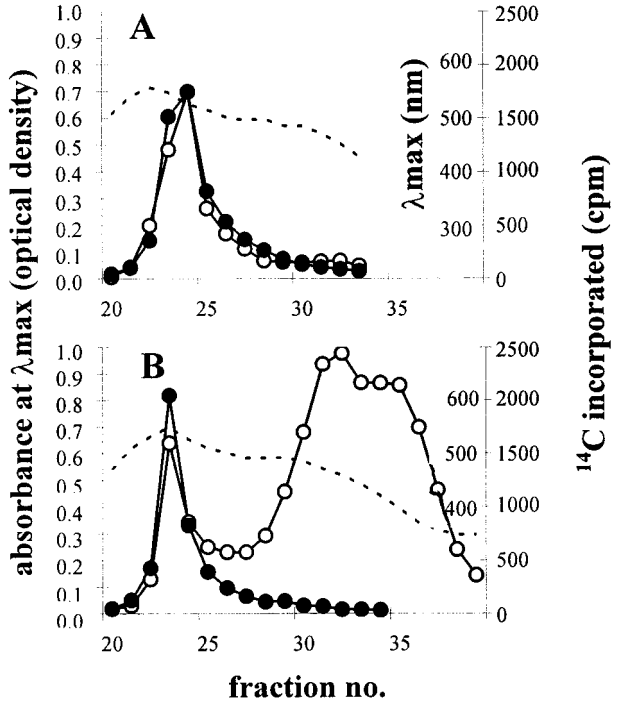

FIG. 2. **Separation of isoamylase debranched glucans by TSKHW-50 chromatography.** Three milligrams of wild-type amylose and amylopectin separated by CL2B-Sepharose chromatography were mixed with 0.05 mg of amylopectin and amylose from the I7 mutant subjected to 24 h of *in vitro* synthesis. After debranching with isoamylase, the amylose (*A*) and amylopectin (*B*) were subjected to TSKHW-50 chromatography. The optical density (○) of the iodine-polysaccharide complex was measured at λ_{max}. The incorporation of ^{14}C from ADP[U-^{14}C]Glc (●) was determined by liquid scintillation counting. Because of the relative abundance of cold wild-type reference polysaccharides, the OD reflects exclusively the wild-type amylopectin and amylose chain-length distribution, whereas the radioactive material represents the *in vitro* synthesized glucans. The λ_{max} is displayed as a *thin dotted line* and is scaled at the *left side* of the *right y axis*.

experiments, we conclude that authentic amylose biosynthesis has been achieved. It must be stressed that this synthesis occurred at the expense of major changes in the structure of amylopectin. The λ_{max} of the iodine-polysaccharide complex of amylopectin increased from 570 to 600 nm (Fig. 1), while debranching analysis (Fig. 2*B*) clearly shows that the label is incorporated in the fraction excluded from TSK-HW50 chromatography. The OD of the intermediate and small chain-length amylopectin fractions (26–39) before and after *in vitro* synthesis were identical, whereas the OD of the long glucan fractions increased dramatically after *in vitro* synthesis (data not shown). We believe these chains to be external as the β-amylolysis limit of amylopectin increased before and after synthesis from 50–55% to 58–63%, respectively. That these chains are covalently bound to amylopectin is confirmed by the fact that all attempts to dissociate them from amylopectin were unsuccessful. These attempts consisted of dispersing starch with aqueous Me_2SO at 100 °C precipitating the chains with ethanol, resuspending the starch in 10 mM NaOH and running columns at various dilutions. We have also submitted the amylopectin to several rounds of Sepharose CL-2B chromatography. Indeed, the long glucan fraction of amylopectin could only be recovered by enzymatic debranching as was reported both by Baba *et al.* (16) and by Denyer *et al.* (17).

Kinetics of Amylose Deposition—Denyer *et al.* (17) have reported that, in the absence of maltooligosaccharides, after 1 h of incubation, amylopectin was the predominant if not only labeled species. Although these results could be confirmed by us, it was furthermore evident that this situation changed dramatically when longer incubations were analyzed. Our results reported above show that after 24 h of incubation more than 40% of the label is incorporated in the amylose fraction. To study amylose deposition, we followed the kinetics of *in vitro* synthesis in the presence of labeled ADP-Glc. For this purpose, we used amylose-less starch granules purified from a nitrogen starved mutant defective for the large subunit of ADP-Glc pyrophosphorylase (22). For each time point, a complete analysis involving Sepharose CL2B chromatography of dissolved starch granules was performed. The OD at λ_{max} and amount of labeled material were thus recorded in each fraction and are displayed in Fig. 3*A* (from 10 min to 2 h) and Fig. 3*B* (from 2 to 24 h). We were thus able to monitor total incorporation of label, as well as the amount selectively synthesized within amylose and amylopectin (Fig. 4). It is clear that *Chlamydomonas*

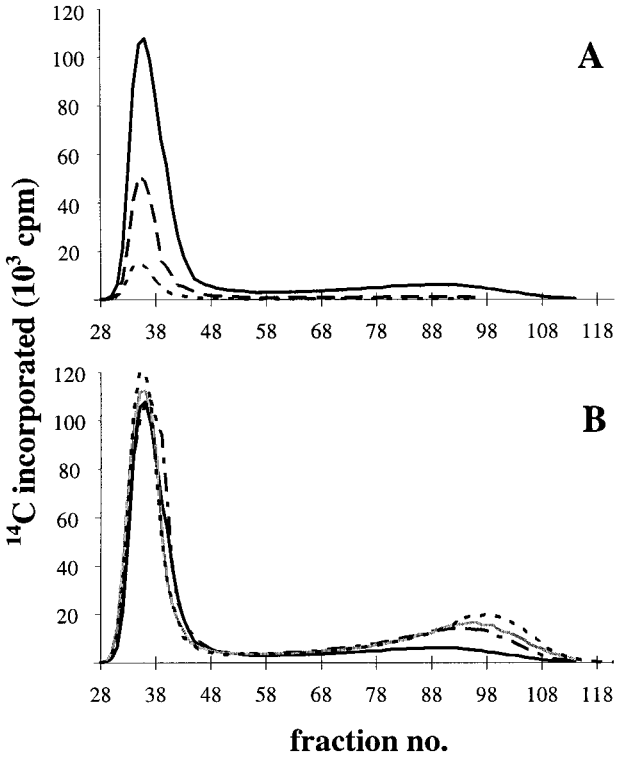

FIG. 3. **Kinetics of *in vitro* synthesis.** Starch from the mutant defective for the large subunit of ADP-Glc pyrophosphorylase (I7) was subjected to *in vitro* synthesis in the presence of ^{14}C- labeled ADP-Glc. After *in vitro* synthesis, the amylopectin and amylose were separated by CL2B-Sepharose chromatography. *A* shows the incorporation of ^{14}C from ADP [U-^{14}C] Glc after 10 min (- - -), 30 min (– – –), and 2 h (——) of *in vitro* synthesis. *B* shows the incorporation of ^{14}C after 2 h (——), 6 h (–·–·–), 12 h (——), and 24 h (- - -). After 2 h, the amount of label incorporated in the amylose fractions increased, whereas there was no further increase in the amount of label incorporated in the amylopectin fractions.

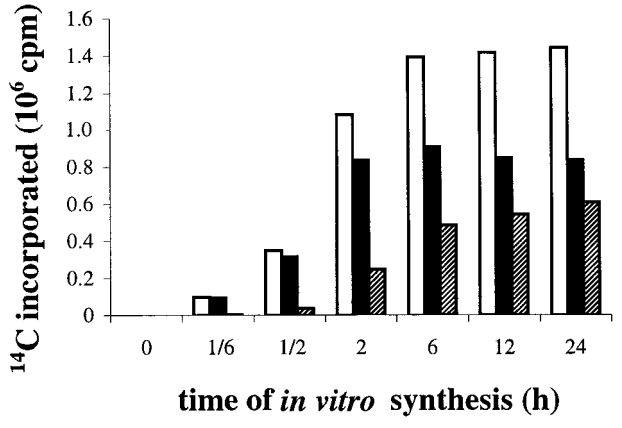

FIG. 4. **Incorporation of ^{14}C from ADP[U-^{14}C]Glc in amylopectin and amylose.** After *in vitro* synthesis in the presence of ^{14}C labeled ADP-Glc, the amylopectin and amylose were separated by CL2B-Sepharose chromatography. The total incorporation of label after different times of *in vitro* synthesis is shown for starch (*white column*), amylopectin (*black column*), and amylose (*gray column*). After 2 h of incubation, amylopectin synthesis was progressively replaced by that of amylose.

starch behaves very much like that of peas in the initial steps. Indeed, very little if any amylose synthesis occurred during the first hour (Fig. 3*A*), while active amylopectin elongation is witnessed. That external amylopectin chains are getting longer is proven by the increase in λ_{max} of the iodine-polysaccharide complex from 570 to 600 nm that is completed within the very first 30 min (Table I). To ascertain that single chains are indeed

TABLE I
λ_{max} of the amylopectin-iodine complex after different times of in vitro synthesis

Wavelength of the maximal absorbance of the iodine polysaccharide complex is expressed in nm.

	Time of *in vitro* synthesis (h)						
	0	1/6	1/2	2	6	12	24
λ_{max}	570	580	600	615	615	610	605

getting longer, we debranched amylopectin and compared the length of these chains to those characterizing mature debranched *C. reinhardtii* amylopectin. Results displayed in Fig. 5 together with our β-amylolysis (see above) studies confirm that external amylopectin chains are getting elongated by GBSSI. Moreover, a bimodal distribution of the long glucans of amylopectin is detected. After 2 h of incubation, amylopectin synthesis becomes progressively substituted by that of amylose (Figs. 3*B* and 4). After 12 h, amylose synthesis rates exceeded those of incorporation by GBSSI. In addition and at the same time, the λ_{max} of the amylopectin-iodine complex is decreasing from 615 to 605 nm (Table I). This result indicates that incorporation in amylose is accomplished at the expense of amylopectin. It is striking to note that high molecular mass amylose biosynthesis occurs before that of the low molecular mass species. thus mimicking the bimodal distribution of the amylopectin external long glucan fractions. At this point of our analysis, we already suspected that external amylopectin chains were used to generate mature amylose by a single endo-type of cleavage event. We thus undertook experiments specifically designed to test this hypothesis.

Pulse-Chase Experiments—The best way to probe the function of amylopectin as a primer for amylose biosynthesis would be to pulse-label the former and check if we can subsequently chase the label into the latter. We chose to pulse-label amylopectin for 30 min at t_0 from starch extracted from the same strain as that was used in the time-course experiments described above. As predicted from our previous experiments, amylopectin was found as the sole labeled species immediately after the radioactive pulse. As synthesis proceeded with unlabeled substrate, the label was slowly but clearly chased into amylose (Fig. 6*A*). Again, the label appeared first in the high molecular mass amylose fraction (Fig. 6*B*). We double-checked that pulse-labeled amylopectin external chains could also be chased into amylose in the case of both transient and storage starches from wild-type algae. An example of such an experiment can be found in Fig. 6*C*, which displays a pulse-chase experiment with storage starch from wild-type algae. Similar pulses gave similar results, yielding a net chase from amylopectin into amylose. In this case, a low but substantial amount of radioactivity in the amylose fraction was immediately detected following the pulse. This result can be simply explained by assuming that a percentage of amylopectin outer chains are already physically ready to be transferred into amylose at t_0. It is worth noting that there again, high molecular mass amylose appears first. Pulse-chase experiments performed on transient starches from wild-type strains behaved in a fashion virtually identical to that which we reported for the low ADP-Glc synthesizing mutants. In addition, during time-course experiments extension of amylopectin chains also preceded the appearance of amylose. Moreover, we double-checked that time-course and pulse-label results obtained from transient starch using 0.5 mM ADP-Glc and pH 7.8 were identical after 4 days of incubation to those obtained after 24 h at 3.2 mM ADP-Glc and pH 8.2. At this stage, the only reasonable interpretation of our results would be to assume that GBSSI extends amylopectin chains. When these chains become "long enough," they are

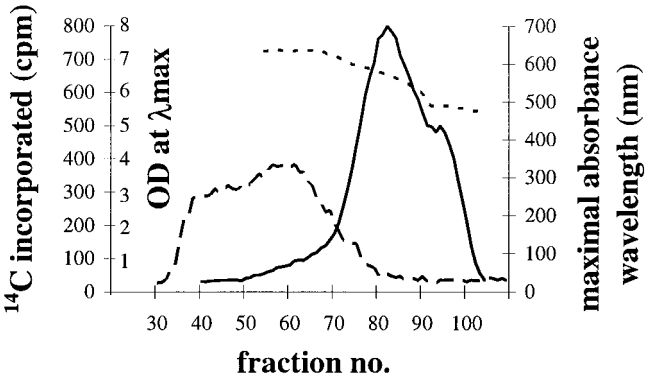

FIG. 5. **Separation of isoamylase debranched amylopectin by CL4B-Sepharose chromatography.** One milligram of wild-type amylopectin separated by CL2B-Sepharose chromatography was mixed with 0.05 mg of amylopectin from the I7 mutant subjected to 1 h of *in vitro* synthesis. After debranching with isoamylase, the amylopectin was subjected to CL4B-Sepharose chromatography. The optical density (——) of the iodine-polysaccharide complex was measured at λ_{max} (- - -). The incorporation of ^{14}C from ADP[U-^{14}C]Glc (– – –) was determined by liquid scintillation counting. Because of the relative abundance of cold wild-type reference polysaccharides, the OD reflects exclusively the wild-type amylopectin chain-length distribution, whereas the radioactive material represents the *in vitro* synthesized glucans. The chains elongated by GBSSI are considerably longer than the average chains of wild-type amylopectin. A bimodal distribution reflecting the existence of two types of external amylopectin chains elongated by GBSSI was already evidenced after 1 h of *in vitro* synthesis.

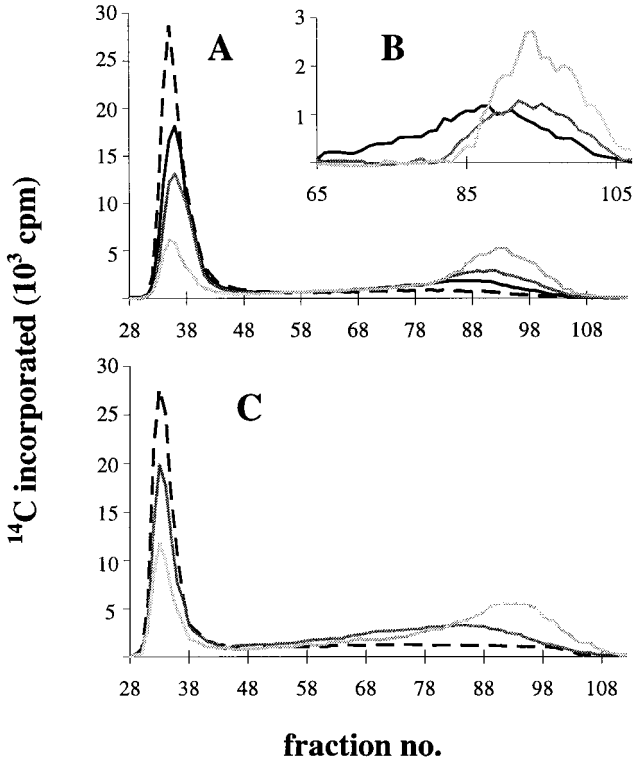

FIG. 6. **Pulse-chase experiment of I7 and wild-type storage starch.** *A* shows the incorporation of ^{14}C from ADP[U-^{14}C]Glc in the mutant defective for the large subunit of ADP-Glc pyrophosphorylase (I7), analyzed with CL2B. After a 30-min pulse-label (*dotted line*), amylopectin was the sole labeled species. After a chase of, respectively, 2 h (*bold black line*), 6 h (*thin black line*), and 24 h (*gray line*), the amount of label incorporated in the amylopectin decreased and the amount of label incorporated in the amylose fraction increased. The label appeared first in the high molecular mass amylose fraction and later in the low molecular mass fraction. This is shown in *B*. The *y axis* in *B* represents the increase in label between the different times and does not represent the total amount of radioactivity. As shown in *A* and *C*, there is no net chase of the high molecular mass material into the low mass material. *C* shows the incorporation of ^{14}C from ADP[U-^{14}C]Glc in wild-type storage starch. After a 30-min pulse-label (*dotted line*), amylopectin was the predominantly labeled species; however, a substantial amount of radioactivity was detected in the amylose fraction. After 6 h (*black line*) and 24 h (*gray line*), a net chase from amylopectin to amylose was detected. Again, high molecular mass amylose appeared first.

released into mature amylose by a single cleavage event. The systematic appearance of high before low molecular mass amylose argues against significant elongation occurring after cleavage. Because we were not entirely satisfied with the meaning of chains "long enough" to be cleaved, we proceeded to search for experimental conditions uncoupling synthesis by GBSSI from that of the postulated cleavage reaction.

Cleavage of Amylose Requires Continuous Chain Elongation and Is Not Stimulated by Maltotriose—In order to uncouple cleavage from synthesis, we used transient starch or storage starch from low ADP-Glc containing mutants. As predicted from our time-course experiments, pulse-labeling for 30 min at t_0 gave incorporation confined to amylopectin. The labeled starch granules were, as usual washed twice, but this time in the absence of any traces of ADP-Glc and in the presence or absence of 50 mM maltotriose. Absence of the substrate blocked cleavage and release into amylose. Because this reaction was not triggered by the presence of 50 mM maltotriose, we reasoned that the previously reported maltooligosaccharide stimulation of amylose synthesis (2, 17) did not seem to involve a selective function of the dextrins on chain termination, at least not on its own. We therefore conclude that chain cleavage is tightly coupled to synthesis through GBSSI.

The Influence of Maltotriose on ^{14}C Incorporation by GBSSI—A number of reports in the literature suggest that amylose biosynthesis is stimulated by addition of maltodextrins such as maltotriose. Therefore, we repeated the experiments performed by Denyer *et al.* (17) using 50 mM maltotriose and 3.2 mM ADP-Glc concentrations. Synthesis of amylose-like material was indeed massive within 1 h of incubation (Fig. 7), whereas relatively little glucose was incorporated in amylopectin. GBSSI incorporated 2–3 times more glucose in the starch granules under these conditions. Two important conclusions can be drawn from this experiment. (i) The approximately 3-fold reduction of label in amylopectin in the presence of maltotriose suggests that the nonreducing ends of maltotriose compete with amylopectin molecules as acceptor substrates. Apparently, a large number of maltotriose molecules have been elongated to such an extent that they became too large too escape from the granule. (ii) The increase in GBSSI activity upon maltotriose supply indicates that the amount of available acceptor substrate in the granule is limiting. This suggests that the immobilized GBSSI cannot use the full potential of nonreducing termini within the starch granule. However, in the presence of a diffusible acceptor substrate such as maltotriose, a larger number of GBSSI molecules can participate in the synthesis reaction. To illustrate the number of nonreducing ends, the following estimation was made. Assuming an amylopectin content of 30%, a volume for one glucose residue of 0.125 nm^3, and an average chain-length of 20 glucose units, we have calculated a nonreducing end concentration of 450 mM within the granule.

The above observations prompted us to investigate ^{14}C incorporation in starch granules with varying ADP-Glc and maltotriose concentrations (Table II). In the absence of maltotriose, ^{14}C incorporation increased proportionally with the ADP-Glc concentration until a concentration of 1 mM is reached. At this stage, the donor substrate concentration was limiting. After this point, the ^{14}C incorporation *versus* ADP-Glc concentration curve started to level off. At an ADP-Glc concentration of 3.2 mM, the incorporation of label increased with the maltotriose

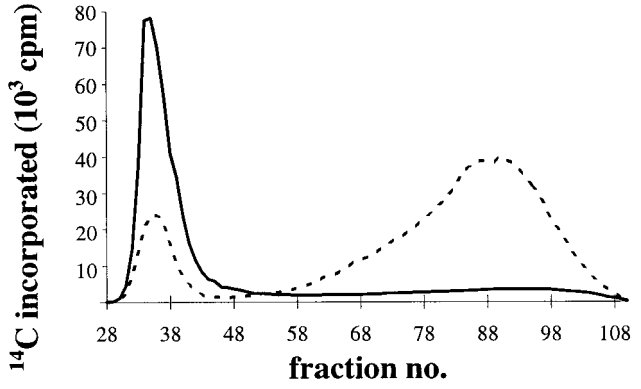

FIG. 7. **Effect of maltooligosaccharides on incorporation of ^{14}C in amylopectin and amylose.** After 1 h of *in vitro* synthesis of I7 starch in the presence of 3.2 mM cold ADP-Glc and 2 μM ADP[U-^{14}C]Glc, the samples were run on a CL2B-Sepharose column. In the absence of 50 mM maltotriose (——), amylopectin was the predominantly labeled species. In the presence of 50 mM maltotriose (- - -), the total amount of radioactivity incorporated doubled, and amylose was the predominantly labeled species.

TABLE II
GBSSI activity at different ADP-Glc and maltotriose concentrations

Activities are expressed as nanomoles of ADP-Glc incorporated into insoluble polysaccharide per minute.

ADP-Glc concentration	Maltotriose concentrations					
	0	2	5	10	50	200
mM	*mM*					
0.01	0.12	0.10	0.09	0.08	0.07	0.06
0.04	0.44	0.49	0.48	0.46	0.39	0.29
0.2	2.0	2.6	2.7	2.7	2.5	2.1
1.0	8.8	10	12	14	14	12
3.2	18	26	33	42	47	43

concentration, until a maltotriose concentration of 50 mM was reached. At 200 mM maltotriose, a reduced ^{14}C incorporation was observed. Because of the abundance of maltotriose, most of the label was transferred to this acceptor molecule instead of to amylopectin. Assuming that small maltodextrins as maltotetraose and maltopentaose dissociate readily from GBSSI, the consequence of a very high maltotriose concentration is that many of these molecules are extended with only a few glucose units. After 1 h of incubation, these molecules had not grown long enough to be retained in the granules upon washing and consequently ^{14}C incorporation was reduced. In fact, this means that the actual GBSSI activity (at least) with 3.2 mM ADP-Glc and 200 mM maltotriose was underestimated. With lower ADP-Glc concentration as well, an "optimal" maltotriose concentration for label incorporation was observed. However, the optimum shifted to lower maltotriose concentrations as expected.

The Consequences of Massive Amylose Biosynthesis on Granule Crystallinity—Our *in vitro* synthesis experiments gave us a unique opportunity to test the impact of massive amylose synthesis in complete absence of concomitant crystalline amylopectin biosynthesis. Crystalline diffraction patterns of plant starches fall into two distinct types, namely the so-called A- and B-types. A-type diffraction patterns are found in cereal endosperm and *C. reinhardtii* starches, whereas the B-type is found in potato tuber and high amylose mutant starches. GBSSI-defective mutants from algae and cereals display the very same A-type patterns. However, high amylose mutants from maize and *C. reinhardtii* switch to the B-type of crystalline organization. Because these high amylose mutants are affected in the amylopectin biosynthesis pathway, it is not known if the switch is due a modification in amylopectin structure or to the

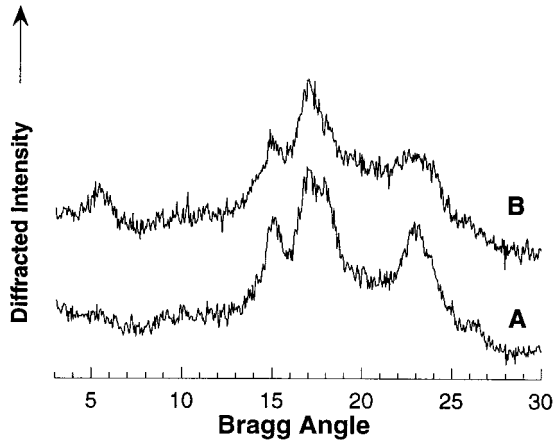

FIG. 8. **Wide angle x-ray diffractograms of starches before and after *in vitro* synthesis of amylose.** The starch x-ray diffractogram before and after 48 h of *in vitro* synthesis are displayed, respectively, in *traces A* and *B*. Diffraction peaks at 2θ (Bragg angle) values of 9.9, 11.2, 15, 17, 18.1, and 23.3° characterize the A-type starches, whereas diffraction peaks at 2θ values of 5.6, 15, 17, 22, and 24° typify B-type starches. It is clear that the t_{48} (*B*) starch sample has switched from the A-type (*A*) to the B-type.

increase in amylose, which by itself could influence the amylopectin crystalline organization. We therefore compared the wide angle x-ray diffraction analysis of a sample of t_0 transient starch with less than 1% in weight amylose to that of the very same starch that was subjected to intensive *in vitro* synthesis for over 48 h with 3.2 mM ADP-Glc leading to 45% final amylose content.

The x-ray diffraction diagrams are displayed in Fig. 8. The crystallinities measured for the t_0 and t_{48} samples amounted to 27 and 16%, respectively. Transient starch displays an A-type diffraction diagram with a crystallinity of about 27%, very close to those described previously for *Chlamydomonas* storage starch (15). After prolonged synthesis, the diagram clearly switched to the B-type with a lower crystallinity (16%). Nevertheless, the degree of crystallinity of B-type starches is well known to depend strongly on the water content (27). Therefore, the calculated value is only relative, as it was not possible to manage the hydration level on a so small amount of substrate. Moreover, some A-type can be still present in t_{48} starch. Indeed, it is impossible in B-type starch diffraction diagrams to detect less than 15% A-type (34), because of the high similarity of spectra and the low crystallinity of native starches.

DISCUSSION

In the present study, we have used both mutant and wild-type *Chlamydomonas* starch granules to elucidate the process of amylose biosynthesis. Comparison of amylose synthesis in these backgrounds with that of starch purified from a strain containing a gene-disrupted GBSSI structural gene showed that only GBSSI enzyme activity was measured under our experimental conditions. We have proven, by pulse-chase experiments among other techniques, that extension of amylopectin external-chains by GBSSI occurs *in vitro* (Table I) with subsequent cleavage into amylose (Fig. 6, *A* and *C*). We have not found evidence for chain elongation within the amylose fraction itself. In addition, we have repeatedly observed a progressive switch from high to low molecular mass amylose synthesis (Fig. 6*B*). Comparison of wild-type and *in vitro* synthesized amylose by CL2B chromatography (Fig. 1*C*), debranching analysis followed by gel permeation chromatography (Fig. 2*A*) and determination of the β-limit dextrin have shown that *in vitro* synthesis yields a branched polymer that is indistinguishable from native amylose. Based on the results described in this

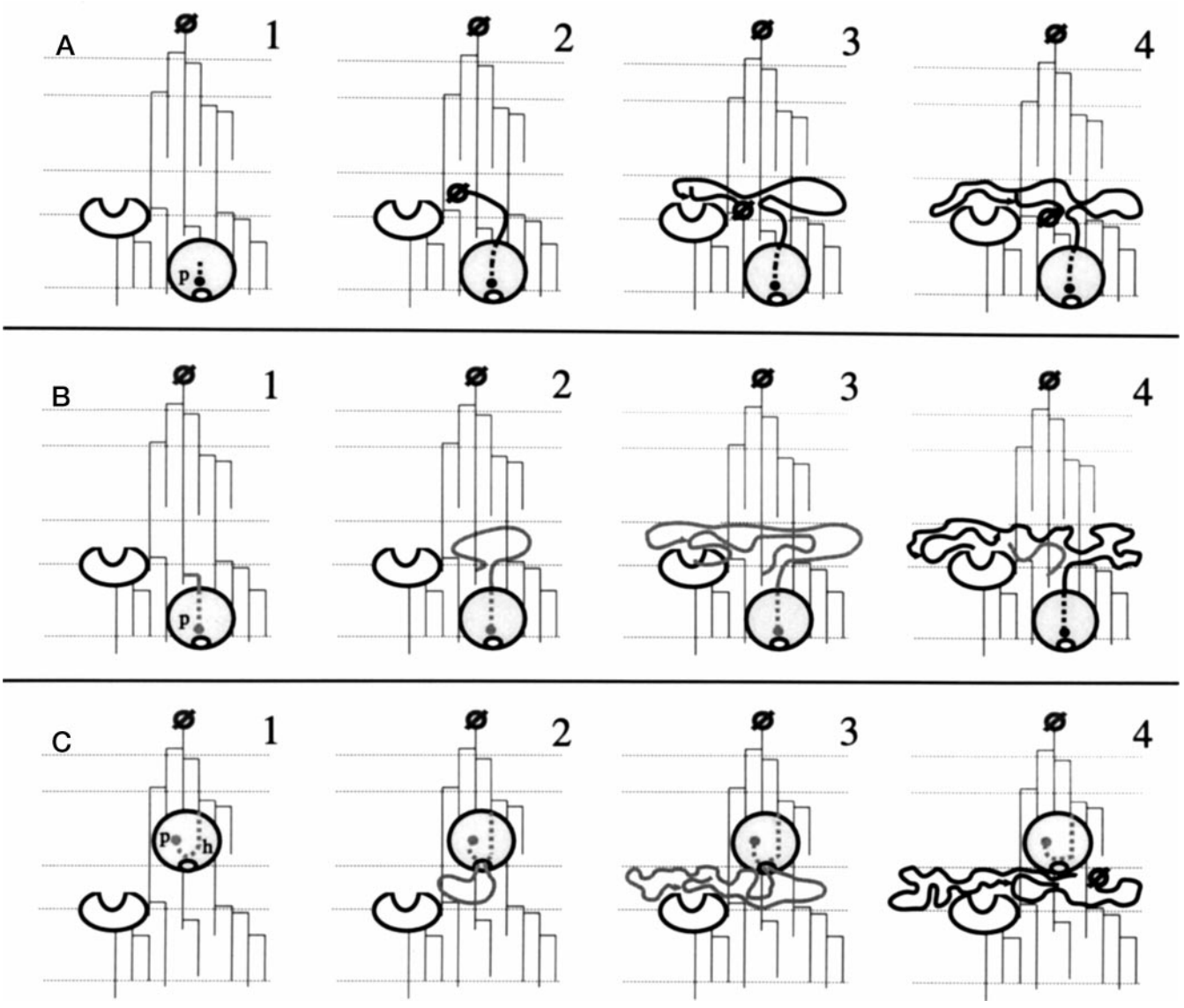

FIG. 9. **Possible models explaining amylose synthesis within the starch granule by immobilized GBSSI.** All reaction steps occur within the very dense polysaccharide matrix inside the granule. The GBSSI is displayed as a *tunnel-shaped* enzyme, whereas branching enzyme is drawn as a *moon-shaped* structure. ● symbolizes a glucan nonreducing end, whereas ∅ symbolizes a reducing end. The catalytic sites of GBSSI are given as "*p*" and "h", indicating a polymerase and a postulated hydrolase activity, respectively. Amylopectin is shown as a *light gray line*, whereas amylose is shown as a *black line*. *A* shows the maltooligosaccharide-primed amylose synthesis, whereas *B* and *C* show the amylopectin-primed amylose biosynthesis. In *B*, we show a BE-mediated cleavage through intra-molecular transglycosylation. Cleavage by a hydrolytic enzyme is also possible but not shown in this figure. In contrast to *B*, *C* shows that hydrolysis (*h*) can occur very near the site of polymerization (*p*) whinin GBSSI, ensuring that a non-reducing end is close to the site of synthesis for reinitiating the next round of amylose biosynthesis.

paper, we propose an entirely new route for amylose biosynthesis.

Active GBSSI can be localized bound at the surface, bound within the granule, or both. The physical location of the active enzyme is of paramount importance because it is only at the surface that the enzyme can eventually be considered as moving with the growing amylose molecules. Within the polysaccharide matrix itself, there is very little room if any for enzyme movement. We have chosen to discuss only the latter possibility. Indeed, evidence for the presence of actively moving and readily dissociating surface enzyme is presently lacking. Three possible models accounting for amylose synthesis within the starch granule are displayed in Fig. 9. The three models share a number of major assumptions, which will be discussed first. We assume that each GBSSI enzyme is tightly bound to the amylopectin matrix and is in fact an immobilized enzyme. Although this assumption remains to be formally proven the resistance of GBSSI activity to proteases, the pronounced decrease of the apparent K_m following solubilization of the enzyme (28) and the immunolocalization of this enzyme within the granule (29) are all in agreement with it. Moreover, we must take into account the inability of large proteins to diffuse into the polysaccharide matrix, the likelihood of amylose deposition within the amorphous cavities of the granule, and the availability of GBSSI for multiple rounds of amylose chain synthesis. Assuming an amylose content of 30%, an average molecular weight of 500,000 (25), and an amount of approximately 2.5 μg of 76-kDa GBSSI protein/mg of starch (estimated by SDS gel electrophoresis), we have calculated a 1:18 ratio of GBSSI to amylose molecules. The major difference between model A on the one hand and models B and C on the other is that the former uses maltooligosaccharides as an acceptor substrate, whereas the latter two use amylopectin. When ADP-Glc is supplied, extension of the polysaccharide chain occurs at the nonreducing end of the molecule pushing the nascent glucan into the amorphous cavities of the granule (Fig. 9). The part of

the glucan situated the furthest away from the nonreducing end of the glucan is more likely to encounter the less abundant branching enzyme (BE) trapped in the granule (Fig. 9). Amylose branching is thus a stochastic event requiring a close encounter with BE within the path of the growing glucan.

We have been able to reproduce the effect of maltooligosaccharides on *in vitro* amylose synthesis previously reported by Denyer *et al.* (17) in our system (Fig. 7). The reduction of label in amylopectin in the presence of maltotriose indicated that high concentrations of maltooligosaccharides compete with amylopectin as acceptor substrate for GBSSI. Incorporation of ^{14}C in the insoluble polysaccharide at different concentrations of ADP-Glc and maltotriose (Table II) suggests that at high ADP-Glc concentrations the length of the glucans produced is long enough to be retained within the granule whereas at lower concentrations the relatively short oligosaccharides will escape from the granule. Such small labeled oligosaccharides were indeed reported by Leloir and colleagues (2) in experiments involving UDP-Glc concentrations well below the apparent K_m of the enzyme. Our present evidence points to normal amylose synthesis occurring in the absence of maltooligosaccharides. After prolonged incubation in the absence of maltooligosaccharides, massive amylose synthesis was achieved whereas our incubation media contained less than 1 μM maltooligosaccharides (data not shown). Whether or not maltooligosaccharide-primed amylose biosynthesis occurs *in vivo* is a matter of available acceptor substrate concentrations. The cluster-like structure of amylopectin provides a formidable potential of nonreducing ends in the starch granule (see "Results"). The increase of ^{14}C incorporation upon addition of diffusible maltooligosaccharides (Table II) strongly indicates that GBSSI cannot use this full potential. However, the large number of possible priming sites within the starch granule, together with the presence of amounts of maltooligosaccharides below 1 mM in wild-type *Chlamydomonas* undergoing amylose biosynthesis, make it very unlikely that maltooligosaccharide priming is important *in vivo*.

Models B and C account for the amylopectin-primed amylose synthesis that we have observed (Fig. 6). In these models, the external amylopectin chain is secured in the active site of GBSSI and we assume that enzyme and substrate do not easily dissociate, due to the immobilized character and processivity of the enzyme and the organized structure of amylopectin. Amylose is formed when the side chain is detached from the amylopectin molecule. Model B suggests that cleavage occurs far from GBSSI, either by BE through an intramolecular transglycosylation (Fig. 9*B*) or by a hydrolytic enzyme trapped within the granule, *e.g.* α-amylase (not indicated in the figure). Takata *et al.* (30, 31) have demonstrated that BE from *Bacillus stearothermophilus* can catalyze inter- and intramolecular branching of both amylose and amylopectin, and they suggest that these reactions are common to BEs from various sources. As a result of the intramolecular transfer by BE, the newly formed amylose will not have a reducing end and is cyclic at the point of cleavage. However, because the number of amylose molecules more or less agrees with the number of reducing ends documented for amylose, we believe that downstream cleavage through hydrolases is presently a more likely hypothesis. Cleavage far from GBSSI implies that the nonreducing end of the amylopectin chain will not be easily available for a next round of synthesis. In this case, multiple rounds of amylose synthesis will depend on the accessibility of new amylopectin nonreducing ends to GBSSI and the possibility of dissociation of the GBSSI-substrate complex. In model C, the assumption is made of an hydrolytic event occurring very near the site of synthesis within GBSSI. We postulate that steric hindrance of the glucan's progress will trigger hydrolysis by the GBSSI enzyme itself, assuming that GBSSI has a dual activity, *i.e.* synthase (or polymerase) and hydrolase. Such a dual activity has been observed before in the Klenow fragment of DNA polymerase of *Escherichia coli*. The N terminus contains a 3′-5′ exonuclease (hydrolase) activity, whereas the C-terminal part contains a polymerase function (32). After release of the amylose chain, the old external amylopectin chain, which has never left the acceptor binding sites, can reinitiate the next round of amylose biosynthesis. In this model, growth of the glucan will be finally stopped by the lack of space within the amylopectin matrix. This will be a late event at the beginning of amylose synthesis and will happen progressively sooner as the starch granule fills with amylose. This can explain why long chain amylose precedes that of the low molecular mass material. Also, the position of GBSSI within the granule can be of influence on the synthesis of low and high molecular mass amylose. Jane and Shen (33) have shown that both concentration and size of amylose is dependent on its position within the starch granule. A detailed biochemical characterization of GBSSI is required to determine whether amylose biosynthesis proceeds via mechanism B or C.

Our results also prove that filling the starch granule with amylose *in vitro* in the absence of concomitant crystalline amylopectin synthesis is sufficient to change the crystalline organization within the granule. There are presently two possibilities to explain these results. First, because of the large amount of amylose present after synthesis, it is possible that the newly synthesized material crystallizes in the B-type under *in vitro* conditions. Another intriguing and perhaps more likely hypothesis would be that the massive amylose synthesis within the amylopectin matrix would push the preexisting A-type into B-type crystals. Indeed, the structure proposed for the B-type crystals displays a central cavity that could be easily filled by one or two amorphous amylose chains (35), whereas the denser A-type packing does not allow for amylose infiltration within the crystal. Our present estimates of crystallinity levels before and after *in vitro* synthesis of amylose do not allow us to discriminate between these two possibilities. However, our results do establish *in vitro* synthesis of amylose from transient *Chlamydomonas* starches as an extremely powerful system to investigate the selective impact of amylose on the structure of amylopectin within the granule.

We believe that the model we propose is useful in that it makes a number of experimentally testable predictions. One of them is that a radioactive pulse given at the time of amylose synthesis should lead to a net chase of radioactive material from amylopectin to amylose. We are thus proceeding to confirm our *in vitro* approach by similar experiments performed *in vivo* in the presence of normal amylopectin synthesis.

Acknowledgments—We thank André Decq, Davy B. Pontoire, and Philippe Dubois for excellent technical assistance. We also thank Paul Colonna for critically reading the manuscript.

REFERENCES

1. Preiss, J., and Sivak, M. N. (1996) in *Photoassimilate Distribution in Plants and Crops: Source-Sink Relationships* (Zamski, E., and Schaffer, A. A., eds) pp. 63–96, Marcel Dekker Inc., New York
2. Leloir, L. F., de Fekete, M. A. R., and Cardini, C. E. (1961) *J. Biol. Chem.* **236,** 636–641
3. Recondo, E., and Leloir, L. (1961) *Biochem. Biophys. Res. Commun.* **6,** 85–88
4. de Fekete, M. A. R., Leloir, L. F., and Cardini, C. E. (1960) *Nature* **187,** 918–919
5. Nelson, O. E., and Rines, H. W. (1962) *Biochem. Biophys. Res. Commun.* **9,** 297–300
6. Weatherwax, P. (1922) *Genetics* **7,** 568–572
7. Murata, T., Sugiyama, T., and Akazawa, T. (1965) *Biochem. Biophys. Res. Commun.* **18,** 371–376
8. Eriksson, G. (1969) *Hereditas* **63,** 180–204

9. Nakamura, T., Yamamori, M., Hirano, H., Hidaka, S., and Nagamine, T. (1995) *Mol. Gen. Genet.* **248,** 253
10. Hovenkamp-Hermelink, J. H. M., Jacobsen, E., Ponstein, A. S., Visser, R. G. F., Vos-Scheperkeuter, G. H., Bijmolt, E. W., de Vries, J. N., Witholt, B., and Feenstra, W. J. (1987) *Theor. Appl. Genet.* **75,** 217–221
11. Denyer, K., Barber, L. M., Burton, R., Hedley, C., Hylton, C., Johnson, S., Jones, D., Marshall, J., Smith, A., Tatge, H., Tomlinson, K., and Wang, T. (1996) *Plant Cell Environ.* **18,** 1019–1026
12. Konishi, Y., Nojima, H., Okuno, K., Asaoka, M., and Fuwa, H. (1985) *Agric. Biol. Chem.* **49,** 1965–1971
13. Delrue, B., Fontaine, T., Routier, F., Decq, A., Wieruszeski, J. M., van den Koornhuyse, N., Maddelein, M. L., Fournet, B., and Ball, S. (1992) *J. Bacteriol.* **174,** 3612–3620
14. Buléon, A., Gallant, D. J., Bouchet, B., Mouille, G., D'Hulst, C., Kossmann, J., and Ball, S. (1997) *Plant Physiol* **115,** 949–957
15. Ponstein, A. S., Oosterhaven, K., Feenstra, W. J., and Witholt, B. (1991) *Starch/Stärke* **43,** 208–220
16. Baba, T., Yoshii, M., and Kainuma K. (1987) *Starch/Stärke* **39,** 52–56
17. Denyer, K., Clarke, B., Hylton, C., Tatge, H., and Smith, A. (1996) *Plant J.* **10,** 1135–1143
18. Maddelein, M. L., Libessart, N., Bellanger, F., Delrue, B., D'Hulst, C., van den Koornhuyse, N., Fontaine, T., Wieruszeski, J. M., Decq, A., and Ball, S. G. (1994) *J. Biol. Chem.* **269,** 25150–25157
19. Fontaine, T., D'Hulst, C., Maddelein, M. L., Routier, F., Marianne-Pepin, T., Decq, A., Wieruszeski, J. M., Delrue, B., van den Koornhuyse, N., Bossu, J. P., Fournet, B., and Ball, S. G. (1993) *J. Biol. Chem.* **268,** 16223–16230
20. Ball, S., Marianne, T., Dirick, L., Fresnoy, M., Delrue, B., and Decq, A. (1991) *Planta* **185,** 17–26
21. Libessart, N., Maddelein, M. L., van den Koornhuyse, N., Decq, A., Delrue, B., and Ball, S. G. (1995) *Plant Cell* **7,** 1117–1127
22. van den Koornhuyse, N., Libessart, N., Delrue, B., Zabawinski, C., Decq, A., Iglesias, A., Carton, A., Preiss, J., and Ball, S. (1996) *J. Biol. Chem.* **271,** 16281–16287
23. Harris, E. H. (ed) (1989) *The Chlamydomonas Sourcebook: A Comprehensive Guide to Biology and Laboratory Use*, pp. 25–63, Academic Press, San Diego
24. Ball, S. G., Dirick, L., Decq, A. Martiat, J. C., and Matagne R. F. (1990) *Plant Sci.* **66,** 1–9
25. Buléon, A., Colonna, P., Planchot, V., and Ball, S. G. (1998) *Int. J. Biol. Macromol.*, in press
26. Wakelin, J. H., Virgin H. S., and Crystal, E. (1959) *J. Appl. Phys.* **30,** 1654–1662
27. Buléon, A., Bizot H., Delage M. M., and Multon J. L. (1982) *Starch/Stärke* **32,** 361–366
28. Macdonald, F. D., and Preiss, J. (1985) *Plant Physiol.* **78,** 849–852
29. Denyer, K., Sidebottom, C., Hylton, C. M., and Smith, A. M. (1993) *Plant J.* **4,** 191–198
30. Takata, H., Takaha, T., Okada, S., Takagi, M., and Imanaka, T. (1996) *J. Bacteriol.* **178,** 1600–1606
31. Takata, H., Takaha, T., Okada, S., Hizukuri, S., Takagi, M., and Imanaka, T. (1996) *Carbohydr. Res.* **295,** 91–101
32. Blanco, L., Bernad, A., Blasco, M. A., and Salas, M. (1991) *Gene* (*Amst.*)**100,** 27–38
33. Jane, J., and Shen, J. J. (1993) *Carbohydr. Res.* **247,** 279–290
34. Planchot, V., Colonna, P., and Buléon, A. (1997) *Carbohydr. Res.* **298,** 319–326
35. Imberty, A., Buleon, A., Tran, V., and Perez, S. (1991) *Starch/Stärke* **43,** 375–384